Am J Physiol Heart Circ Physiol 313: H190–H199, 2017.
First published May 5, 2017; doi:10.1152/ajpheart.00117.2017.

RESEARCH ARTICLE | *Cardiac Excitation and Contraction*

Sarcolemmal distribution of I_{Ca} and I_{NCX} and Ca^{2+} autoregulation in mouse ventricular myocytes

Hanne C. Gadeberg, Cherrie H. T. Kong, Simon M. Bryant, Andrew F. James, and Clive H. Orchard
School of Physiology, Pharmacology and Neuroscience, University of Bristol, Bristol, United Kingdom

Submitted 17 February 2017; accepted in final form 1 May 2017

Gadeberg HC, Kong CH, Bryant SM, James AF, Orchard CH. Sarcolemmal distribution of I_{Ca} and I_{NCX} and Ca^{2+} autoregulation in mouse ventricular myocytes. *Am J Physiol Heart Circ Physiol* 313: H190–H199, 2017. First published May 5, 2017; doi:10.1152/ajpheart.00117.2017.—The balance of Ca^{2+} influx and efflux regulates the Ca^{2+} load of cardiac myocytes, a process known as autoregulation. Previous work has shown that Ca^{2+} influx, via L-type Ca^{2+} current (I_{Ca}), and efflux, via the Na^+/Ca^{2+} exchanger (NCX), occur predominantly at t-tubules; however, the role of t-tubules in autoregulation is unknown. Therefore, we investigated the sarcolemmal distribution of I_{Ca} and NCX current (I_{NCX}), and autoregulation, in mouse ventricular myocytes using whole cell voltage-clamp and simultaneous Ca^{2+} measurements in intact and detubulated (DT) cells. In contrast to the rat, I_{NCX} was located predominantly at the surface membrane, and the hysteresis between I_{NCX} and Ca^{2+} observed in intact myocytes was preserved after detubulation. Immunostaining showed both NCX and ryanodine receptors (RyRs) at the t-tubules and surface membrane, consistent with colocalization of NCX and RyRs at both sites. Unlike I_{NCX}, I_{Ca} was found predominantly in the t-tubules. Recovery of the Ca^{2+} transient amplitude to steady state (autoregulation) after application of 200 μM or 10 mM caffeine was slower in DT cells than in intact cells. However, during application of 200 μM caffeine to increase sarcoplasmic reticulum (SR) Ca^{2+} release, DT and intact cells recovered at the same rate. It appears likely that this asymmetric response to changes in SR Ca^{2+} release is a consequence of the distribution of I_{Ca}, which is reduced in DT cells and is required to refill the SR after depletion, and NCX, which is little affected by detubulation, remaining available to remove Ca^{2+} when SR Ca^{2+} release is increased.

NEW & NOTEWORTHY This study shows that in contrast to the rat, mouse ventricular Na^+/Ca^{2+} exchange current density is lower in the t-tubules than in the surface sarcolemma and Ca^{2+} current is predominantly located in the t-tubules. As a consequence, the t-tubules play a role in recovery (autoregulation) from reduced, but not increased, sarcoplasmic reticulum Ca^{2+} release.

cardiac myocytes; t-tubules; autoregulation, L-type calcium current; sodium/calcium exchange current

T-TUBULES are invaginations of the surface membrane of cardiac ventricular myocytes that play a central role in excitation-contraction coupling. Contraction is initiated by Ca^{2+} influx [Ca^{2+} current (I_{Ca})] through L-type Ca^{2+} channels (LTCCs); this activates ryanodine receptors (RyRs) in the adjacent sarcoplasmic reticulum (SR) membrane to cause Ca^{2+} release from the SR [Ca^{2+}-induced Ca^{2+} release (CICR)]. I_{Ca}, RyRs, and thus CICR occur predominantly at t-tubules (6, 8, 14), which results in a near-synchronous rise in cytosolic Ca^{2+} throughout the cell to levels sufficient to activate the contractile proteins.

For myocytes to relax, Ca^{2+} must be removed from the cytosol. This is achieved by Ca^{2+} reuptake into the SR and Ca^{2+} efflux from the cell. Although SR Ca^{2+} uptake is the main route of Ca^{2+} removal from the cytosol, sarcolemmal Ca^{2+} efflux pathways, the Na^+/Ca^{2+} exchanger (NCX) and sarcolemmal Ca^{2+} ATPase, also play an important role (1, 25). Evidence largely from rat cardiac myocytes suggests that, like influx, Ca^{2+} efflux also occurs predominantly at the t-tubules (11, 14, 37) where, it has been proposed, NCX has privileged access to Ca^{2+} released from the SR (2, 20, 41).

The balance between sarcolemmal Ca^{2+} influx and efflux determines the Ca^{2+} load of the cell and thus the amplitude of the Ca^{2+} transient and is maintained by a process called "autoregulation," which involves regulation of both Ca^{2+} influx and efflux by cytoplasmic Ca^{2+}. For example, sensitizing CICR has only a short-lived effect on the Ca^{2+} transient amplitude (17, 39, 42) because the resulting increase in SR Ca^{2+} release decreases I_{Ca} by Ca^{2+}-dependent inactivation of I_{Ca} and increases Ca^{2+} efflux by stimulating NCX (17, 36). These changes reduce the Ca^{2+} transient amplitude back to baseline levels with an accompanying decrease in SR Ca^{2+} content (17, 39, 42). The role of t-tubules in autoregulation is unknown; however, because I_{Ca} and its inactivation by Ca^{2+} as well as NCX current (I_{NCX}) and its stimulation by Ca^{2+} released from the SR have been reported to occur predominantly at the t-tubules (6, 14, 30), it seems likely that they play an important role in autoregulation. Therefore, this study was designed to determine the sarcolemmal distribution of I_{Ca} and I_{NCX} and the consequences for the role of the t-tubules in autoregulation in mice.

MATERIALS AND METHODS

Myocyte isolation and detubulation. Ventricular myocytes were isolated from the hearts of male C57BL/6 mice aged between 11 and 13 wk. All procedures were performed in accordance with United Kingdom legislation and approved by the University of Bristol Ethics Committee. Mice were injected with heparin (500 IU by intraperitoneal injection) and killed by cervical dislocation. The heart was excised and washed in isolation solution supplemented with 0.1 mM $CaCl_2$ and 10 U/ml heparin. The heart was then Langendorff perfused with isolation solution for 4 min followed by enzyme solution (isolation solution plus 0.1 mM $CaCl_2$, 265 U/ml collagenase, and 0.3 U/ml protease) for ~15 min. The ventricles were then removed and shaken in enzyme solution for 4–6 min before being filtered and centrifuged. Cells were resuspended in isolation solution (pH 7.4) plus

Address for reprint requests and other correspondence: C. H. Orchard, School of Physiology, Pharmacology and Neuroscience, Biomedical Sciences Bldg., Univ, of Bristol, Bristol BS8 1TD, UK (e-mail: clive.orchard@bristol.ac.uk).

  ISSN 0363-6135.

0.1 mM $CaCl_2$ and stored for 2–8 h before use on the day of isolation. Detubulation (DT), the physical and functional uncoupling of the t-tubules from the surface membrane, was achieved using formamide-induced osmotic shock, as previously described, by incubating cells with 1.5 M formamide for 2 min before centrifugation and resuspending the cells in Tyrode solution (5). Data from intact and DT myocytes were obtained from separate groups of cells.

Chemicals and solutions. All reagents were obtained from Sigma-Aldrich (Poole, UK) unless otherwise specified. The isolation solution contained (in mM) 130 NaCl, 5.4 KCl, 0.4 NaH_2PO_4, 4.2 HEPES, 10 glucose, 1.4 $MgCl_2$, 20 taurine, and 10 creatine (pH 7.6 using NaOH). Tyrode solution used for experiments contained (in mM) 133 NaCl, 1 $MgSO_4$, 1 $CaCl_2$, 1 Na_2HPO_4, 10 D-glucose, and 10 HEPES (pH 7.4 using NaOH) plus 5 CsCl to inhibit K^+ currents. The pipette solution contained (in mM) 100 CsCl, 20 TEACl, 10 NaCl, 0.5 $MgCl_2$, 5 MgATP, 10 HEPES, 0.4 GTP-Tris (pH 7.2 using CsOH), and 0.1 pentapotassium salt of the fluorescent Ca^{2+} indicator fluo-4 (Life Technologies, Paisley, UK).

Measurement of membrane currents. Myocytes were placed in a chamber mounted on a Diaphot inverted microscope (Nikon UK, Kingston-upon-Thames, UK). Membrane currents and cell capacitance were recorded using the whole cell patch-clamp technique using an Axopatch 200B patch-clamp amplifier, a Digidata 1440A analog-to-digital converter, and pClamp 10 software (Molecular Devices, Reading, UK), which was also used for data acquisition (at 2 kHz) and analysis. Pipette tip resistances were typically 1.2–2.0 MΩ when filled with pipette solution. All experiments were performed at room temperature.

To monitor Ca^{2+} influx and efflux, and thus Ca^{2+} balance, during a Ca^{2+} transient, holding potential was set to −80 mV; a 500-ms ramp to −40 mV was used to inactivate Na^+ current followed by step depolarization to 0 mV for 100 ms to activate I_{Ca} at a frequency of 1 Hz. I_{Ca} was measured as the difference between peak inward current and current at the end of the pulse to 0 mV, and the integral was taken as a measure of Ca^{2+} influx. Inactivation of I_{Ca} was quantified by measuring the time to 50% inactivation ($T_{50\%}$). The current representing Ca^{2+} removed by NCX after the step depolarization ($I_{NCX,tail}$) was measured by fitting a single-exponential function to 350 ms of the current trace starting 20 ms after repolarization from 0 to −80 mV and extrapolating back to when the membrane was repolarized. The integral of the exponential was taken as a measure of Ca^{2+} efflux during the Ca^{2+} transient (13, 15). This analysis was performed using MATLAB R2015a (Mathworks, Natick, MA).

To determine the distribution of I_{NCX} between the surface and t-tubule membranes, I_{NCX} was measured in intact and DT myocytes during the application of 10 mM caffeine to cause spatially and temporally uniform release of SR Ca^{2+} (4); the resulting inward current due to Ca^{2+} extrusion via NCX was recorded at −80 mV, and I_{NCX} was taken as the difference between the peak current and the current after caffeine washout.

The distribution of I_{Ca}, I_{NCX}, and membrane capacitance (a function of membrane area), and, thus, current density, between the surface and t-tubular membranes was calculated from measurements in intact (whole cell) and DT (surface membrane only) myocytes, as previously described (7, 8). In brief, the currents and capacitance of the surface sarcolemma were calculated from those measured in DT myocytes, corrected for incomplete DT assessed using confocal imaging of Di-8-ANEPPS-stained cells as 12.7%; t-tubular currents and capacitance were calculated from the difference between those in intact cells and those in the surface sarcolemma.

Measurement of intracellular Ca^{2+}. Fluo-4 fluorescence was excited at 450–488 nm, and emitted fluorescence was collected at wavelengths <560 nm. Fluorescence was normalized to fluorescence just before application of caffeine (F/F_0). The rate of decay of Ca^{2+} transients was obtained by fitting single exponential functions to the declining phase of the I_{Ca}- and caffeine-induced Ca^{2+} transients.

Analysis of NCX hysteresis loops. NCX hysteresis loops were produced by plotting I_{NCX} against F/F_0 during application of 10 mM caffeine to release SR Ca^{2+}, as previously described (14, 41). Loops were quantified by calculating the area within the loop and normalizing to the rectangle defined by maximum and minimum I_{NCX} and F/F_0 (41).

Immunocytochemistry. Cells were fixed with 4% paraformaldehyde for 10 min before being permeabilized with 0.1% Triton X-100 and stained with primary antibodies for RyR (MA3-916, Thermo Fisher) or NCX (R3F1, Swant) overnight. Cells were then incubated in Alexa fluor 488-conjugated anti-mouse secondary antibody before being mounted with ProLong Gold. Cells were imaged on an LSM 880 confocal microscope (Zeiss) in Airyscan "super-resolution" mode, with a 1.4 numerical aperture ×63 oil-immersion objective.

Staining at the cell surface and in the center of the cell was determined from a binary cell image obtained using Otsu's method (27). The perimeter of the cell was outlined manually, and staining within a band that extended 2 μm inside this outline was taken as the cell edge; staining from the image inside this band, excluding the nuclei, was taken as the cell center.

Staining was quantified as follows:

$$\text{Normalized staining density} = \frac{\%\text{bright pixels}}{\%\text{total pixels}} \quad (1)$$

where %bright pixels is the percentage of bright pixels in a given area relative to the total number of bright pixels in the cell and %total pixels is the percentage of pixels in a given area relative to the total number of pixels in the cell.

Statistical analysis. Data are expressed as means ± SE. Errors of derived variables (e.g., t-tubule I_{Ca} and I_{NCX} densities) and the subsequent statistical analysis were calculated using propagation of errors from the constituent measurements (8). Student's *t*-tests and two-way ANOVA with the Bonferroni post hoc test were used as appropriate and performed using GraphPad Prism 7 (GraphPad Software, San Diego, CA). The limit of statistical confidence was $P < 0.05$. All statistical tests were performed on the number of cells. Sample sizes (*n* numbers) are given as *c*/*h*, where *c* is the number of cells used from *h* number of hearts.

Autoregulation model. The mathematical model of autoregulation described by Eisner et al. (12) was used to simulate the data obtained in intact and DT myocytes. Baseline values for intact cells were those used by Eisner et al. (12) except that the transsarcolemmal Ca^{2+} efflux fraction (*r*) was decreased from 10% to 8% (the value measured in the current experiments). The relative changes obtained experimentally in DT cells were used to model the data in these cells: I_{Ca} was decreased from 10 to 4.1, fractional SR Ca^{2+} release (*f*) was decreased from 0.7 to 0.287, and *r* was maintained at 8%, the value measured in DT cells. Changes in I_{NCX} relative to steady state obtained from the experimental data were incorporated for intact and DT myocytes.

RESULTS

I_{NCX} distribution in mouse ventricular cells. DT significantly decreased cell capacitance from 181 ± 9 (n = 28/13) to 128 ± 6 pF (n = 24/11, $P < 0.0001$), with no change in cell volume, calculated as previously described previously (3) [54 ± 4 pl (intact) vs. 58 ± 4 pl (DT)]. After correction for incomplete DT, this suggests that 41% of the cell membrane is t-tubular.

I_{NCX} was measured in intact and DT myocytes during application of 10 mM caffeine to determine its distribution. Figure 1 shows representative records of intracellular Ca^{2+}, monitored as fluo-4 fluorescence, and the associated I_{NCX} in intact (Fig. 1*A*) and DT (Fig. 1*B*) myocytes during application of caffeine. DT had no significant effect on either the ampli-

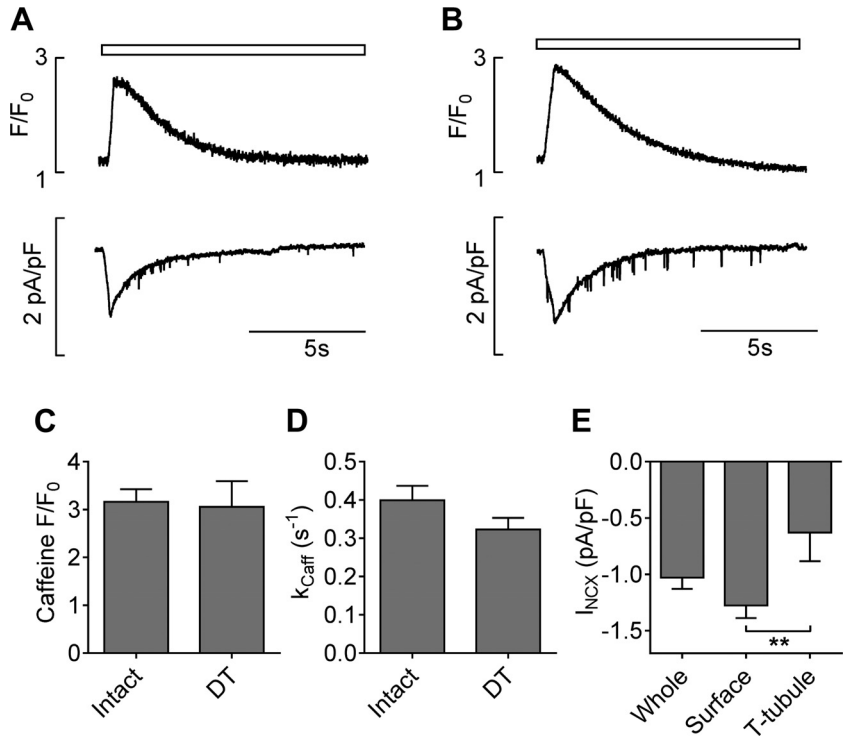

Fig. 1. Representative caffeine-induced Ca^{2+} transients (*top*) and corresponding Na^+/Ca^{2+} exchanger (NCX) current (I_{NCX}) densities (*bottom*) in intact (*A*) and detubulated (DT; *B*) myocytes. Caffeine application is indicated by the open bars at top. The bar charts show the means ± SE of caffeine-induced Ca^{2+} transient amplitude (*C*), rate of decay (k_{Caff}; *D*), and I_{NCX} density distribution (*E*). Intact: n = 14/7; DT: n = 10/7. $^{**}P < 0.01$.

tude or rate of decay (k_{Caff}) of the caffeine-induced Ca^{2+} transient (Fig. 1, *C* and *D*), suggesting that SR Ca^{2+} content and sarcolemmal Ca^{2+} efflux are unchanged by DT of mouse cells. Figure 1*E* shows whole cell I_{NCX} density and the calculated density of I_{NCX} at the surface and t-tubular membranes, showing that the density of I_{NCX} in the t-tubules is about half that in the surface membrane ($P < 0.01$). Thus, ~25% of total I_{NCX} appears to occur in the t-tubules, consistent with the small, although statistically nonsignificant, decrease in mean k_{Caff} on DT (Fig. 1*D*).

Previous work in rat ventricular myocytes has shown that when caffeine is applied to release Ca^{2+} from the SR, I_{NCX} is greater for a given cytoplasmic Ca^{2+} concentration as Ca^{2+} increases than during the subsequent decrease. It has been suggested that this hysteresis arises because Ca^{2+} released from the SR has "privileged" access to NCX due to the proximity of NCX to RyRs. Thus, during Ca^{2+} release, NCX is responding to a higher local Ca^{2+} concentration than that reported by a Ca^{2+} indicator in the cytoplasm, while during the falling phase, the local Ca^{2+} concentration surrounding NCX is closer to bulk cytoplasmic Ca^{2+} concentration (41). Hysteresis is lost after DT in rat ventricular myocytes, consistent with the hysteresis arising at the t-tubules as a result of localization of I_{NCX} to the t-tubules, close to the site of Ca^{2+} release, in these cells (14, 41). Because the majority of I_{NCX} appears to be located at the surface sarcolemma in mouse ventricular myocytes, we investigated whether the hysteresis and its response to DT were different in these cells by plotting I_{NCX} against F/F_0. Figure 2*A* shows that intact cells showed a marked hysteresis that was not abolished by DT: I_{NCX} density for a given Ca^{2+} was greater during the rising phase than the declining phase of the caffeine-induced transient in both cell types, with no significant difference in the area ratio of the loop (see Fig. 2*B* and MATERIALS AND METHODS). However, the loop was shifted in DT cells, with a greater I_{NCX} density for a given Ca^{2+}, consistent with a similar Ca^{2+} release but greater I_{NCX} density at the cell surface. These data are consistent with the majority of NCX being located at the surface sarcolemma in the mouse and the location of I_{NCX} determining the hysteresis, which arises at the site of highest I_{NCX} density: the t-tubules in the rat and the surface sarcolemma in the mouse.

NCX and RyR distribution. Immunohistochemistry was used to investigate the distribution of NCX and RyR. Figure 2*C* shows confocal images of a representative mouse myocyte stained for NCX, showing marked striations within the cell and continuous staining at the cell surface, consistent with NCX being present at the t-tubular and surface membranes and thus with the measured distribution of I_{NCX}. Figure 2*D* shows a representative cell stained for RyRs, which showed marked striations, consistent with t-tubular localization, with less staining at the cell surface, although two or sometimes three distinct areas of RyRs were observed coinciding with the mouth of t-tubules (Fig. 2*D*,*ii*). Staining of NCX and RyRs at the cell edge and cell center, quantified using *Eq. 1*, are shown in Fig. 2*E*; the apparent density of NCX staining was higher than that of RyR at the cell surface ($P < 0.0001$, Bonferroni post hoc test) but similar in the cell center, although both proteins had a greater density at the cell edge than at the cell center ($P < 0.0001$, two-way ANOVA). However, although the images were obtained using Airyscan "super-resolution" to minimize the contribution of out of focus light, there may be more surface membrane than t-tubular membrane in the optical field, since the former is likely to be present in the full depth of the field. This could lead to a higher apparent NCX density at the cell surface, although its effect on measured RyR density is unclear. However, although quantification is difficult, these data show that Ca^{2+} release sites and NCX are present at the

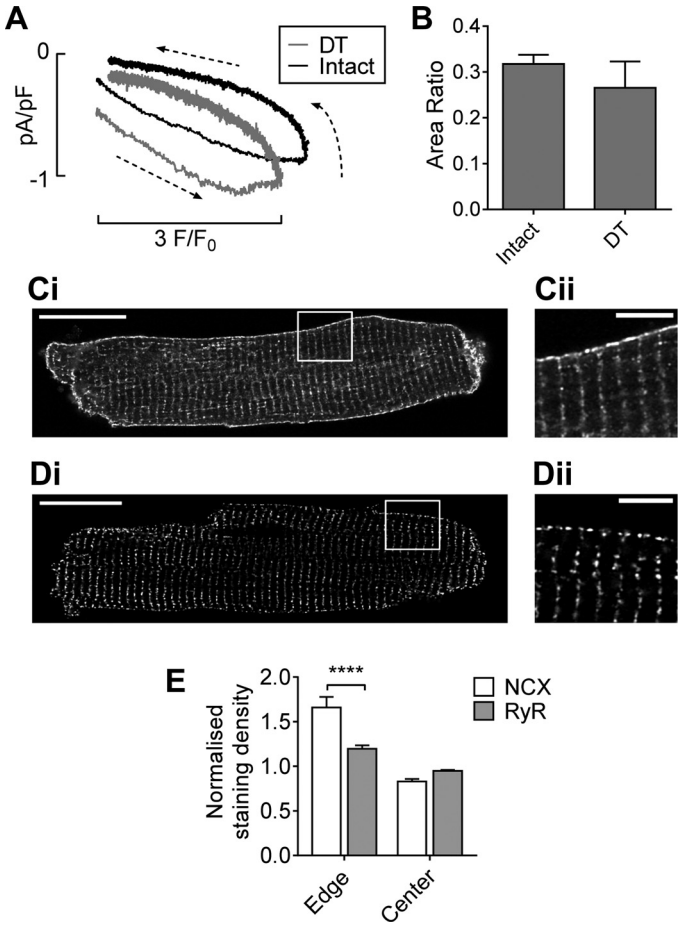

Fig. 2. *A*: average hysteresis loops in intact (black; $n = 14/7$) and DT (gray; $n = 10/7$) myocytes. Membrane current is shown relative to that at the end of the application of caffeine in intact myocytes. *B*: mean (±SE) hysteresis area ratios. *C* and *D*: Representative confocal images of NCX (*C*) and ryanodine receptor (RyR; *D*) staining of a whole cell (*i*), with the area indicated shown at higher magnification in *ii*. Scale bars = 20 μm and 5 μm for low- and high-magnification images, respectively. *E*: NCX and RyR staining at the edge and center of the cell calculated according to *Eq. 1*. ****$P < 0.0001$ with the Bonferroni post hoc test.

cell edge, consistent with the observed distribution of I_{NCX} and the hysteresis observed in DT myocytes.

I_{Ca} distribution in mouse ventricular cells. Since I_{NCX} distribution appears to be different in mouse and rat myocytes, we also investigated the distribution of I_{Ca} in these cells. Figure 3 shows representative I_{Ca} and the elicited Ca^{2+} transients in intact (Fig. 3*A*) and DT (Fig. 3*B*) myocytes. Consistent with previous reports in rat myocytes, the Ca^{2+} transient amplitude (Fig. 3*C*) and rate of decay (Fig. 3*D*) were significantly decreased by DT (5, 6, 21).

I_{Ca} in intact and DT cells was used to calculate the distribution of I_{Ca} between the surface sarcolemma and t-tubule membranes. Figure 3*E* shows that I_{Ca} density was about four times greater in the t-tubule membrane compared with the surface sarcolemma ($P < 0.0001$), as in the rat (6, 8, 14). However, in contrast to the rat, there was no significant change in the rate of inactivation of I_{Ca} after DT (Fig. 3*F*), suggesting that inactivation was similar at the surface and t-tubular membranes.

Effect of DT on Ca^{2+} autoregulation. Since the distribution of Ca^{2+}-handling proteins determines the role of the t-tubules in Ca^{2+} handling (4, 6, 14, 38), we investigated the effect of detubulation on the recovery of systolic Ca^{2+} transient amplitude and Ca^{2+} flux via I_{Ca} and I_{NCX} after depletion of SR Ca^{2+} by a high concentration (10 mM) of caffeine, and during and after application of a low concentration (200 μM) of caffeine to sensitize CICR (26, 42), both of which elicit autoregulation.

Figure 4 shows that after application of 10 mM caffeine, Ca^{2+} transient amplitude was initially small and gradually recovered to steady state with successive beats in both intact (Fig. 4*A*,*i*) and DT (Fig. 4*B*,*i*) myocytes. Recovery was accompanied by a decrease in the amplitude and integral of I_{Ca}, and an increase in the amplitude and integral of I_{NCX} in both intact (Fig. 4*A*,*ii*) and DT (Fig. 4*B*,*ii*) myocytes. However, steady-state Ca^{2+} transient amplitude was significantly smaller in DT cells ($P < 0.0001$), consistent with reduced I_{Ca} and loss of t-tubules, and the half-time ($t_{1/2}$) to reach steady state was significantly longer (8.7 ± 1.0 s for intact cells vs. 12.6 ± 0.4 s for DT cells, $P < 0.01$); thus, the rate of recovery due to SR refilling was slower in DT myocytes (Fig. 4*C*). Figure 4*D* shows that recovery of Ca^{2+} transient amplitude was accompanied by a small reduction in Ca^{2+} influx via I_{Ca} in both intact and DT cells, although Ca^{2+} influx, and thus the rate of Ca^{2+} accumulation, was significantly smaller in DT myocytes (Fig. 4, *D* and *E*). In contrast, Ca^{2+} efflux via I_{NCX} gradually increased with continued stimulation in both cell types (Fig. 4*F*), reflecting an increase in SR Ca^{2+} content and release, although Ca^{2+} efflux was significantly smaller in DT cells (Fig. 4, *F* and *G*), which is likely to reflect the decrease in Ca^{2+} transient amplitude due to reduced I_{Ca} rather than loss of NCX (above).

The ratio between Ca^{2+} influx and efflux was calculated to compare Ca^{2+} balance in intact and DT cells (Fig. 4*H*). In both cell types, the ratio was initially greater than 1 after caffeine, reflecting net Ca^{2+} influx, and gradually decreased toward 1, which represents the steady-state balance of influx and efflux. However, the initial ratio was slightly lower in DT than intact myocytes. These data suggest that reduced Ca^{2+} influx via I_{Ca}, and therefore slower Ca^{2+} accumulation, underlies the slower recovery of Ca^{2+} transient amplitude in DT cells and thus that the t-tubules play an important role in autoregulation.

To test this idea further, Ca^{2+} autoregulation was investigated during application and washout of 200 μM caffeine to intact (Fig. 5*A*) and DT (Fig. 5*B*) myocytes. Application of caffeine to intact myocytes caused a transient increase in Ca^{2+} transient amplitude, which recovered to steady state, while washout of caffeine caused a transient decrease in Ca^{2+} transient amplitude, which also recovered to steady state, consistent with previous work (e.g., Ref. 39). DT cells showed a similar response, although the Ca^{2+} transient amplitude was smaller; mean data are shown in Fig. 5*C*. Interestingly, the half-time to recover to steady state during application of caffeine was not changed by DT (5.7 ± 0.7 s in intact cells vs. 5.3 ± 0.6 s in DT cells), but the recovery to steady state on washout of caffeine was significantly slowed in DT cells ($t_{1/2}$: 3.1 ± 0.3 s in intact cells vs. 5.4 ± 0.4 s in DT cells, $P < 0.001$), similar to the recovery after 10 mM caffeine.

Application of 200 μM caffeine caused similar changes in the rate of inactivation of I_{Ca} in intact and DT myocytes (Fig. 5*D*) and decreased Ca^{2+} influx in both cell types, whereas

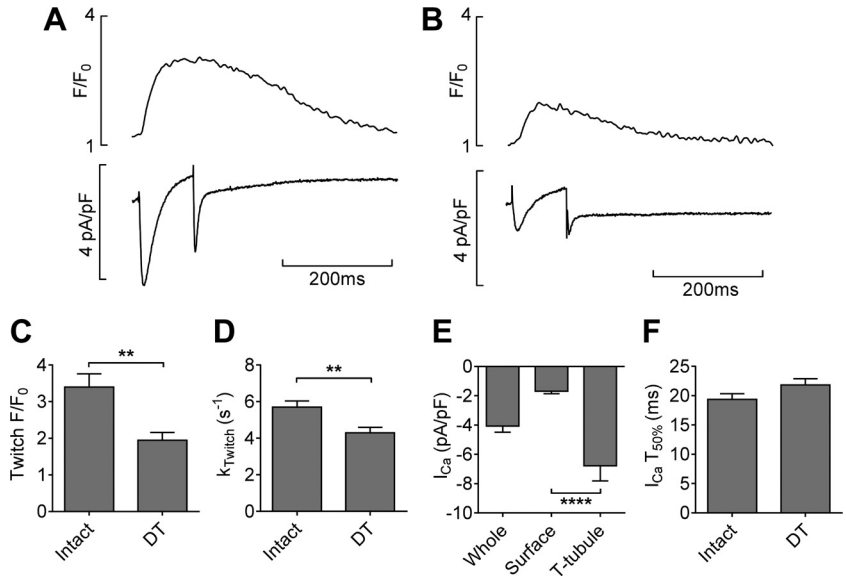

Fig. 3. Representative Ca^{2+} current (I_{Ca})-stimulated Ca^{2+} transients (*top*) and the corresponding I_{Ca} and current representing Ca^{2+} removed by NCX after the step depolarization ($I_{NCX,tail;}$ *bottom*) in intact (*A*) and DT (*B*) myocytes. The bar charts show corresponding means (±SE) for Ca^{2+} transient amplitude (*C*), k_{Twitch} (*D*), I_{Ca} density distribution (*E*), and half-time ($T_{50\%}$) of I_{Ca} inactivation (*F*). Intact: n = 14/7; DT: n = 10/7. $^{**}P < 0.01$; $^{****}P < 0.0001$.

washout caused only a small increase in both cell types (Fig. 5*E*). Ca^{2+} efflux increased on application of 200 μM caffeine, while on washout efflux was reduced (Fig. 5*F*). Although both influx and efflux were significantly ($P < 0.001$) reduced in DT cells, the overall balance was not significantly different (Fig. 5*G*), whether during application 200 μM caffeine, where the balance favored Ca^{2+} efflux, or whether during washout of caffeine, where the balance favored net Ca^{2+} influx.

Taken together, these data suggest that t-tubules play an important role in recovery from a decrease in SR Ca^{2+} load, since DT cells recover more slowly, but not in recovery from an increased SR Ca^{2+} release, since intact and DT cells recover at similar rates. To test this idea further, we incorporated the data from intact and DT myocytes into the model of Eisner et al. (12), as described in MATERIALS AND METHODS. The results of these simulations are shown in Fig. 6, which shows that after SR Ca^{2+} depletion (Fig. 6*A*), DT cells recovered much more slowly than intact cells ($t_{1/2}$: 10.7 stimuli in intact cells vs. 26.8 stimuli in DT cells), as observed experimentally (cf. Fig. 4*C*). In contrast, the rate of recovery during sensitization of CICR (Fig. 6*B*) was similar in intact and DT myocytes ($t_{1/2}$: 8.8 stimuli in intact cells vs. 12.8 stimuli in DT cells), consistent with the data from the experiments (cf. Fig. 5*C*).

DISCUSSION

The present study was designed to investigate the role of the t-tubules in Ca^{2+} autoregulation in mouse ventricular myocytes. The data show that the majority of I_{Ca} occurs in the t-tubules, whereas, in contrast to rat myocytes, I_{NCX} occurs mainly at the surface sarcolemma and the hysteresis between Ca^{2+} and I_{NCX} persists after DT. Although autoregulation to steady state occurred after DT, the time course of recovery was slower during recovery from decreased SR Ca^{2+} release but, interestingly, not from increased SR Ca^{2+} release. This suggests that t-tubules play a role in recovery from decreased, but not increased, SR Ca^{2+} release, which may reflect the localization of I_{Ca} and I_{NCX}.

Distribution of I_{Ca} and I_{NCX} in the mouse sarcolemma. Previous work has shown that I_{Ca} and I_{NCX} occur predominantly in the t-tubules in rat ventricular myocytes (6, 8, 11, 14, 21, 37, 44). The present study demonstrated a slightly higher t-tubular membrane fraction (41%) than that previously reported for rat myocytes (6, 8, 30), consistent with the higher t-tubule density reported previously for the mouse (18, 29); it also showed that I_{Ca} is located predominantly in the t-tubules of mouse myocytes, consistent with a previous report using DT in mouse myocytes (19). The presence of I_{Ca} at the t-tubules in both species, in close proximity to the majority of RyRs, allows the tight coupling between Ca^{2+} influx and SR Ca^{2+} release that underlies CICR, while the higher t-tubule density in the mouse may reflect its high heart rate and the consequent need for rapid activation.

However, the present work also demonstrated that, in contrast to rat ventricular myocytes, I_{NCX} is located predominantly at the cell surface in mouse myocytes. Although this might explain some of the discrepancies in the literature regarding the location of NCX determined using immunological techniques (35, 37), it is unclear why the distribution of I_{NCX} should be different in the two species, which have similar Ca^{2+}-handling properties, with similar action potential configurations, fractions of SR and trans-sarcolemmal Ca^{2+} flux (1, 10, 22, 25), and kinetics of contraction and relaxation (23), although computer modeling suggests that NCX distribution has relatively little effect on whole cell Ca^{2+} handling (31). One possibility is that location of NCX at the cell surface is energetically favorable, which might be important at the higher heart rates in the mouse, because it will avoid the futile Ca^{2+} cycling that results from NCX being in close proximity to the main site of SR Ca^{2+} release, by decreasing the amount of released Ca^{2+} that is immediately removed via NCX, enabling more of the released Ca^{2+} to activate the contractile proteins. The small t-tubular I_{NCX} is, however, associated with a small (nonsignificant) decrease in the rate of decay of the caffeine-induced Ca^{2+} transient after DT in the mouse, in contrast to the marked decrease observed in the rat (14).

This species difference in the sarcolemmal distribution of Ca^{2+}-handling protein function raises questions about the distribution in other species. Although, as far as we are aware,

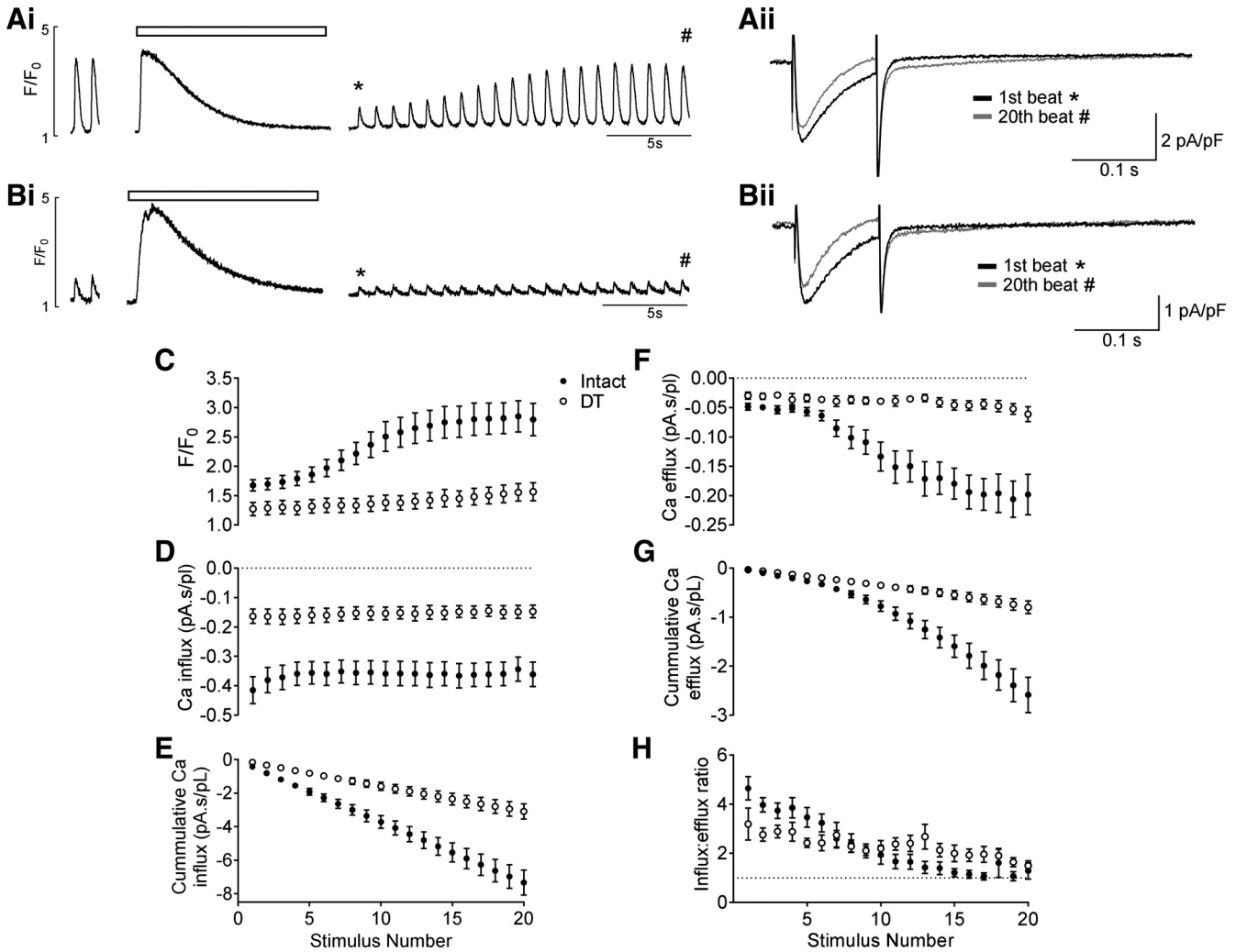

Fig. 4. Representative traces showing recovery of the systolic Ca^{2+} transient after application of 10 mM caffeine (shown by the open bars) in intact (*A*,*i*) and DT (*B*,*i*) myocytes. Representative currents for the first (*) and 20th (#) beat are shown in *ii*. *C*: mean Ca^{2+} transient amplitude. DT was significantly different from intact from the 8th stimulus ($P < 0.05$) to the 20th stimulus ($P < 0.001$). *P* values here and subsequently represent the results of a Bonferroni post hoc test. *D*: mean Ca^{2+} influx. DT was significantly different from intact from the 1st stimulus ($P < 0.0001$) to 20th stimulus ($P < 0.01$). *E*: mean cumulative Ca^{2+} influx. DT was significantly different from intact from the 9th stimulus ($P < 0.05$) to 20th stimulus ($P < 0.0001$). *F*: mean Ca^{2+} efflux. DT was significantly different from intact from the 10th stimulus ($P < 0.05$) to 20th stimulus ($P < 0.0001$). *G*: mean cumulative Ca^{2+} efflux. DT was significantly different from intact from the 10th stimulus ($P < 0.05$) to 20th stimulus ($P < 0.0001$). *H*: mean Ca^{2+} influx-to-efflux ratio. *C*–*H*: all during recovery after caffeine. Intact: $n = 14/7$; DT: $n = 10/7$.

corresponding data are not available for large mammals, previous work in cultured guinea pig myocytes (28) showed no significant change in I_{NCX} density with time in culture, whereas cell capacitance decreased (correlating with loss of t-tubules), suggesting a similar I_{NCX} density in the surface sarcolemma and t-tubules of guinea pig myocytes (28). Nevertheless, the maintained I_{NCX} density might have been due to other mechanisms upregulating I_{NCX} in culture.

It has been suggested that the hysteresis between I_{NCX} and bulk cytoplasmic Ca^{2+} is due to the proximity of NCX to the site of Ca^{2+} release, so that the exchanger responds to a higher Ca^{2+} concentration than monitored in the bulk cytosol during Ca^{2+} release. The hysteresis is abolished after DT of rat myocytes (14), suggesting that this occurs at the t-tubules, where the majority of NCX is located close to the site of SR Ca^{2+} release, and that surface sarcolemmal I_{NCX} responds mainly to changes in global Ca^{2+} concentration. The present observation that the hysteresis is present in both intact and DT mouse myocytes is consistent with the observed distribution of I_{NCX} in these cells and suggests that I_{NCX} at the surface sarcolemma is located close to sites of Ca^{2+} release and responding to local changes of Ca^{2+} concentration during Ca^{2+} release (and to changes in global Ca^{2+} concentration during the descending phase). The staining data support this idea: RyRs were observed not only in striations in the cell interior, consistent with localization at the t-tubules, but also at the surface membrane in clusters at the mouth of t-tubules, close to NCX, which, in agreement with the I_{NCX} measurements, was also observed at both the t-tubules and cell surface. These data suggest that RyRs, and thus Ca^{2+} release, occur at the t-tubules and cell surface and thus that it is the distribution of I_{NCX} that determines the site of the hysteresis in these cells. These data also suggest that the site of origin of arrhythmogenic delayed afterdepolarizations, which are caused by acti-

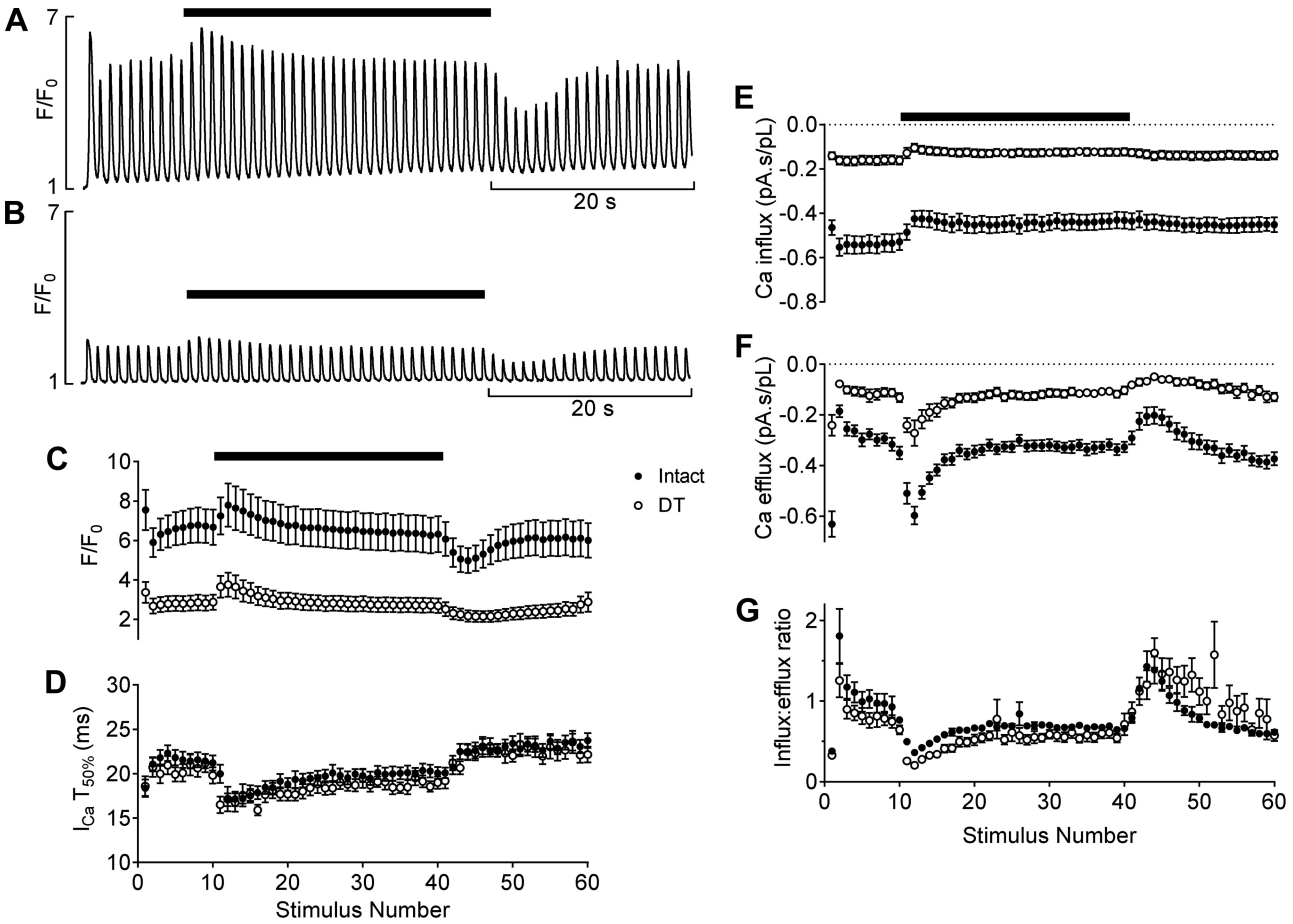

Fig. 5. Representative traces showing systolic Ca^{2+} transients before, during, and after application of 200 μM caffeine (shown by solid bar) in intact (*A*) and DT (*B*) myocytes. *C*: mean Ca^{2+} transient amplitude. DT was significantly different from intact on the 1st stimulus ($P < 0.01$), from the 4th to 10th stimulus ($P < 0.05$), 12th to 35th stimulus ($P < 0.05$), 37th ($P < 0.05$), 50th to 53rd stimulus ($P < 0.05$), and 55th and 56th stimulus ($P < 0.05$). *P* values here and subsequently represent the results of a Bonferroni post hoc test. *D*: mean $T_{50\%}$ of inactivation of I_{Ca}. *E*: mean Ca^{2+} influx. DT was significantly different from intact for all stimuli ($P < 0.0001$). *F*: mean Ca^{2+} efflux. DT was significantly different from intact for all stimuli (ranging from $P < 0.01$ to $P < 0.0001$) except the 2nd stimulus (not significant). *G*: mean Ca^{2+} influx-to-efflux ratio. DT was significantly different from intact for the 2nd stimulus ($P < 0.01$) and 52nd stimulus ($P < 0.001$). *C–G*: all showing before, during, and after application of 200 μM caffeine (indicated by solid bar). Intact: $n = 13/6$; DT: $n = 10/4$.

vation of I_{NCX} by SR Ca^{2+} release, will depend on the location of I_{NCX} and Ca^{2+} release and may thus be different in different species.

Effects of DT on autoregulatory mechanisms. The present data show that, in agreement with previous studies in other species (17, 39), recovery of Ca^{2+} transient amplitude following altered SR Ca^{2+} release is associated with reciprocal changes in Ca^{2+} influx via I_{Ca} and Ca^{2+} efflux via NCX.

Changes in Ca^{2+} transient amplitude result in changes in Ca^{2+} influx through Ca^{2+}-dependent inactivation of I_{Ca}. In rabbit cells, Ca^{2+} influx can increase by 50–60% in the absence of SR Ca^{2+} release (16, 33); in the rat, Ca^{2+} influx can double after SR Ca^{2+} depletion (40). Although Ca^{2+}-dependent inactivation also occurs in mouse myocytes, as seen by the faster inactivation during application of 200 μM caffeine and slower inactivation on wash off in the present study, only small differences in the rate of inactivation between intact and DT myocytes were observed. This suggests, in contrast to rat myocytes in which Ca^{2+}-dependent inactivation occurs predominantly at the t-tubules (6), that inactivation is similar at the surface and t-tubular membranes. The reason for this species difference is unknown but may reflect differences in local Ca^{2+} and/or local LTCC regulation at the two sites. The lack of change in the rate of inactivation of I_{Ca} after DT, despite the smaller Ca^{2+} transient, could be explained by the absence of basal Ca^{2+}-dependent inactivation of I_{Ca} or by rapid inactivation, which is manifested as a change in peak I_{Ca} rather than its duration. However, studies using intracellular Ca^{2+} chelators or barium as the charge carrier for I_{Ca} to inhibit Ca^{2+}-induced inactivation have suggested that there is substantial basal I_{Ca} inactivation, which mainly affects the rate of inactivation rather than peak I_{Ca} (32, 34, 43), making these explanations unlikely. Thus, the most likely cause for I_{Ca} inactivation being unaffected by DT appears to be that local Ca^{2+} release, and thus inactivation, at the cell surface is similar to that at the t-tubules. In this case, the smaller, slower Ca^{2+} transient in DT myocytes is due to loss of the quantitatively more important t-tubular CICR and loss of synchronization of Ca^{2+} release. A similar local Ca^{2+} release at the cell surface and t-tubules can explain why the hysteresis occurs in DT myocytes given the observed distribution of I_{NCX}. Thus, it appears that, in contrast to the rat, both I_{NCX} density and

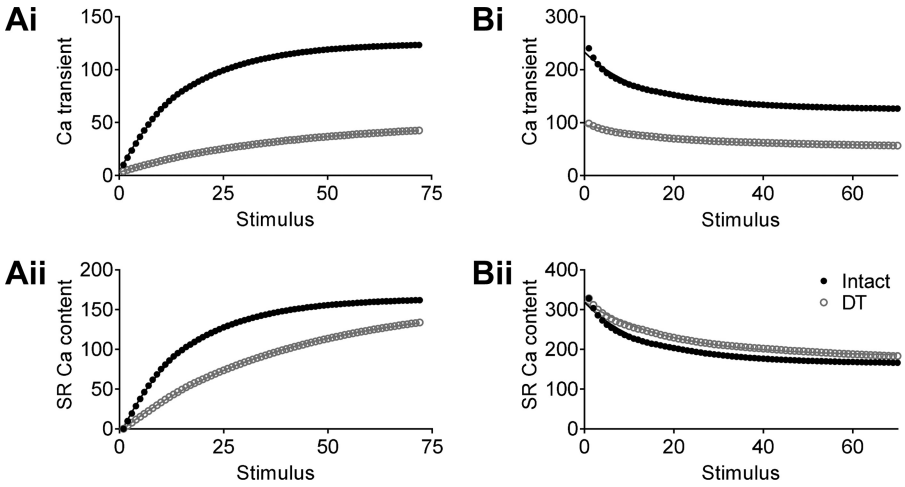

Fig. 6. Effect of incorporating the data from intact and DT myocytes into the model of Eisner et al., showing the effects of detubulation on autoregulation. Shown is the recovery of the Ca^{2+} transient (*i*) and sarcoplasmic reticulum (SR) Ca^{2+} content (*ii*) after depletion of SR Ca^{2+} (*A*) and during sensitization of Ca^{2+}-induced Ca^{2+} release (*B*).

Ca^{2+}-dependent inactivation of I_{Ca} are similar at the t-tubular and surface membranes and that the decrease in Ca^{2+} influx after DT is predominantly due to loss of t-tubular I_{Ca} rather than an altered rate of inactivation.

In contrast to I_{Ca}, regulation of I_{NCX} appears similar to that previously reported, with an increase in I_{NCX} associated with an increase in Ca^{2+} transient amplitude in intact and DT myocytes. DT resulted in changes in k_{Caff} and I_{NCX} consistent with loss of the t-tubular fraction of I_{NCX} (25%), while the hysteresis between I_{NCX} and cytosolic Ca^{2+} showed a larger current for a given Ca^{2+} in DT myocytes, with no loss of hysteresis, consistent with the greater density of I_{NCX} in the surface membrane and similar Ca^{2+} release at the surface and t-tubular membranes. Thus, the observed changes are consistent with the observed distribution of I_{NCX}, with no evidence for altered regulation.

Effects of DT on autoregulation. As in previous studies (4, 14), DT had no effect on SR Ca^{2+} content, as assessed by releasing SR Ca^{2+} using 10 mM caffeine, but did result in a smaller and slower voltage-stimulated Ca^{2+} transient, due to decreased I_{Ca} and thus CICR and loss of synchronization of SR Ca^{2+} release. The smaller Ca^{2+} transient, in turn, decreased I_{NCX}, even though it was present at the surface sarcolemma.

Although DT had no effect on the rate of recovery of Ca^{2+} transient amplitude to steady state when SR Ca^{2+} release was increased using low-dose caffeine, recovery was slower from a decreased SR Ca^{2+} content after caffeine-induced SR Ca^{2+} depletion or on washout of 200 μM caffeine. This asymmetric response to changes in SR Ca^{2+} release in DT cells was not due to the nonlinear response of fluo-4 to Ca^{2+} because it was still present after the conversion of fluorescence to Ca^{2+} (not shown), an idea supported by the model. It may, however, be explained by the differential distribution of I_{Ca} and I_{NCX}. In this case, when an increase in SR Ca^{2+} release occurs, Ca^{2+} efflux via NCX is the main mechanism to decrease Ca^{2+} transient amplitude and return the cell to steady state; thus, in DT mouse cells, in which the majority of I_{NCX} occurs at the surface, recovery is similar in intact and DT myocytes and is not affected by the loss of I_{Ca}. However, when SR Ca^{2+} release is decreased, Ca^{2+} influx via I_{Ca} is necessary to refill the SR and increase Ca^{2+} transient amplitude to steady state and is thus essential for recovery. Since steady-state SR Ca^{2+} content is similar in intact and DT myocytes but Ca^{2+} influx via I_{Ca} is smaller in DT cells, more stimuli are required to refill the SR to steady state, so that recovery is slower in DT than in intact cells, even though the majority of NCX is present and quantitatively shows greater changes over time than I_{Ca}. Slowing of recovery from caffeine has also been reported after DT of rat myocytes (4), consistent with a key role for I_{Ca}, which, like I_{NCX}, occurs predominantly in the t-tubules in this species.

Although t-tubules uncoupled from the surface membrane by DT may reseal within the cell and, in principle, sequester and release Ca^{2+} (5, 24), it seems unlikely that they can explain the current data, since they are electrically uncoupled from the surface membrane. Therefore, Ca^{2+} channels in such resealed tubules will not undergo activation (and thus inactivation), an idea supported by the lack of Ca^{2+} release in the center of DT myocytes (5). Because they do not release Ca^{2+} and have a small volume, they are also unlikely to take up Ca, and previous work inhibiting surface NCX in DT rat myocytes during application of caffeine showed that only ~2% of Ca^{2+} removal occurs into non-SR sinks within the cell (9), which includes mitochondria, and this is likely to be even less in mouse myocytes, which have a smaller fraction of NCX within the t-tubules. Thus, resealed t-tubules are unlikely to play an important role in normal Ca^{2+} cycling or autoregulation, an idea supported by the effects of DT on the Ca^{2+} transient and autoregulation.

Thus, it appears that the t-tubules play an important role in autoregulation in mouse myocytes during recovery from decreased SR Ca^{2+} release, because of the high t-tubular I_{Ca} density, but play little role in the recovery from increased Ca^{2+} release. These data also suggest that the response of a particular species to such changes will depend on the distribution of I_{Ca} and I_{NCX} between the t-tubules and surface sarcolemma. Although the distribution of Ca^{2+} fluxes in human myocytes is unknown, the current work shows that the distribution of I_{Ca} and I_{NCX} determines cell function and enhances our understanding of how this occurs. Thus, when human data become available, it should be possible to better predict the consequent changes in cell function in both physiological conditions and after t-tubule disruption and changes in the distribution of I_{Ca} and I_{NCX}, which have been reported in heart failure (14) and which may also affect autoregulation.

GRANTS

This work was supported by British Heart Foundation Grants PG/14/65/31055 and RG/12/10/29802.

DISCLOSURES

No conflicts of interest, financial or otherwise, are declared by the authors.

AUTHOR CONTRIBUTIONS

H.C.G. performed experiments; H.C.G. and C.H.K. analyzed data; H.C.G., S.M.B., A.F.J., and C.H.O. interpreted results of experiments; H.C.G. prepared figures; H.C.G. and C.H.O. drafted manuscript; H.C.G., C.H.K., S.M.B., A.F.J., and C.H.O. edited and revised manuscript; A.F.J. and C.H.O. conceived and designed research; A.F.J. and C.H.O. approved final version of manuscript.

REFERENCES

1. **Bassani JW, Bassani RA, Bers DM.** Relaxation in rabbit and rat cardiac cells: species-dependent differences in cellular mechanisms. *J Physiol* 476: 279–293, 1994. doi:10.1113/jphysiol.1994.sp020130.
2. **Bovo E, de Tombe PP, Zima AV.** The role of dyadic organization in regulation of sarcoplasmic reticulum Ca^{2+} handling during rest in rabbit ventricular myocytes. *Biophys J* 106: 1902–1909, 2014. doi:10.1016/j.bpj.2014.03.032.
3. **Boyett MR, Frampton JE, Kirby MS.** The length, width and volume of isolated rat and ferret ventricular myocytes during twitch contractions and changes in osmotic strength. *Exp Physiol* 76: 259–270, 1991. doi:10.1113/expphysiol.1991.sp003492.
4. **Brette F, Despa S, Bers DM, Orchard CH.** Spatiotemporal characteristics of SR Ca^{2+} uptake and release in detubulated rat ventricular myocytes. *J Mol Cell Cardiol* 39: 804–812, 2005. doi:10.1016/j.yjmcc.2005.08.005.
5. **Brette F, Komukai K, Orchard CH.** Validation of formamide as a detubulation agent in isolated rat cardiac cells. *Am J Physiol Heart Circ Physiol* 283: H1720–H1728, 2002. doi:10.1152/ajpheart.00347.2002.
6. **Brette F, Sallé L, Orchard CH.** Differential modulation of L-type Ca^{2+} current by SR Ca^{2+} release at the T-tubules and surface membrane of rat ventricular myocytes. *Circ Res* 95: e1–e7, 2004. doi:10.1161/01.RES.0000135547.53927.F6.
7. **Brette F, Sallé L, Orchard CH.** Quantification of calcium entry at the T-tubules and surface membrane in rat ventricular myocytes. *Biophys J* 90: 381–389, 2006. doi:10.1529/biophysj.105.069013.
8. **Bryant SM, Kong CHT, Watson J, Cannell MB, James AF, Orchard CH.** Altered distribution of I_{Ca} impairs Ca release at the t-tubules of ventricular myocytes from failing hearts. *J Mol Cell Cardiol* 86: 23–31, 2015. doi:10.1016/j.yjmcc.2015.06.012.
9. **Chase A, Orchard CH.** Ca efflux via the sarcolemmal Ca ATPase occurs only in the t-tubules of rat ventricular myocytes. *J Mol Cell Cardiol* 50: 187–193, 2011. doi:10.1016/j.yjmcc.2010.10.012.
10. **Choi HS, Eisner DA.** The role of sarcolemmal Ca^{2+}-ATPase in the regulation of resting calcium concentration in rat ventricular myocytes. *J Physiol* 515: 109–118, 1999. doi:10.1111/j.1469-7793.1999.109ad.x.
11. **Despa S, Brette F, Orchard CH, Bers DM.** Na/Ca exchange and Na/K-ATPase function are equally concentrated in transverse tubules of rat ventricular myocytes. *Biophys J* 85: 3388–3396, 2003. doi:10.1016/S0006-3495(03)74758-4.
12. **Eisner DA, Trafford AW, Díaz ME, Overend CL, O'Neill SC.** The control of Ca release from the cardiac sarcoplasmic reticulum: regulation versus autoregulation. *Cardiovasc Res* 38: 589–604, 1998. doi:10.1016/S0008-6363(98)00062-5.
13. **Fedida D, Noble D, Shimoni Y, Spindler AJ.** Inward current related to contraction in guinea-pig ventricular myocytes. *J Physiol* 385: 565–589, 1987. doi:10.1113/jphysiol.1987.sp016508.
14. **Gadeberg HC, Bryant SM, James AF, Orchard CH.** Altered Na/Ca exchange distribution in ventricular myocytes from failing hearts. *Am J Physiol Heart Circ Physiol* 310: H262–H268, 2016. doi:10.1152/ajpheart.00597.2015.
15. **Giles W, Shimoni Y.** Slow inward tail currents in rabbit cardiac cells. *J Physiol* 417: 447–463, 1989. doi:10.1113/jphysiol.1989.sp017812.
16. **Grandi E, Morotti S, Ginsburg KS, Severi S, Bers DM.** Interplay of voltage and Ca-dependent inactivation of L-type Ca current. *Prog Biophys Mol Biol* 103: 44–50, 2010. doi:10.1016/j.pbiomolbio.2010.02.001.
17. **Greensmith DJ, Galli GLJ, Trafford AW, Eisner DA.** Direct measurements of SR free Ca reveal the mechanism underlying the transient effects of RyR potentiation under physiological conditions. *Cardiovasc Res* 103: 554–563, 2014. doi:10.1093/cvr/cvu158.
18. **Heinzel FR, Bito V, Volders PGA, Antoons G, Mubagwa K, Sipido KR.** Spatial and temporal inhomogeneities during Ca^{2+} release from the sarcoplasmic reticulum in pig ventricular myocytes. *Circ Res* 91: 1023–1030, 2002. doi:10.1161/01.RES.0000045940.67060.DD.
19. **Horiuchi-Hirose M, Kashihara T, Nakada T, Kurebayashi N, Shimojo H, Shibazaki T, Sheng X, Yano S, Hirose M, Hongo M, Sakurai T, Moriizumi T, Ueda H, Yamada M.** Decrease in the density of t-tubular L-type Ca^{2+} channel currents in failing ventricular myocytes. *Am J Physiol Heart Circ Physiol* 300: H978–H988, 2011. doi:10.1152/ajpheart.00508.2010.
20. **Jayasinghe I, Crossman D, Soeller C, Cannell M.** Comparison of the organization of T-tubules, sarcoplasmic reticulum and ryanodine receptors in rat and human ventricular myocardium. *Clin Exp Pharmacol Physiol* 39: 469–476, 2012. doi:10.1111/j.1440-1681.2011.05578.x.
21. **Kawai M, Hussain M, Orchard CH.** Excitation-contraction coupling in rat ventricular myocytes after formamide-induced detubulation. *Am J Physiol Heart Circ Physiol* 277: H603–H609, 1999.
22. **Li L, Chu G, Kranias EG, Bers DM.** Cardiac myocyte calcium transport in phospholamban knockout mouse: relaxation and endogenous CaMKII effects. *Am J Physiol Heart Circ Physiol* 274: H1335–H1347, 1998.
23. **Milani-Nejad N, Janssen PM.** Small and large animal models in cardiac contraction research: advantages and disadvantages. *Pharmacol Ther* 141: 235–249, 2014. doi:10.1016/j.pharmthera.2013.10.007.
24. **Moench I, Lopatin AN.** Ca^{2+} homeostasis in sealed t-tubules of mouse ventricular myocytes. *J Mol Cell Cardiol* 72: 374–383, 2014. doi:10.1016/j.yjmcc.2014.04.011.
25. **Negretti N, O'Neill SC, Eisner DA.** The relative contributions of different intracellular and sarcolemmal systems to relaxation in rat ventricular myocytes. *Cardiovasc Res* 27: 1826–1830, 1993. doi:10.1093/cvr/27.10.1826.
26. **O'Neill SC, Eisner DA.** A mechanism for the effects of caffeine on Ca^{2+} release during diastole and systole in isolated rat ventricular myocytes. *J Physiol* 430: 519–536, 1990. doi:10.1113/jphysiol.1990.sp018305.
27. **Otsu N.** A threshold selection method from gray-level histograms. *IEEE Trans Syst Man Cybern* 9: 62–66, 1979. doi:10.1109/TSMC.1979.4310076.
28. **Pabbathi VK, Zhang YH, Mitcheson JS, Hinde AK, Perchenet L, Arberry LA, Levi AJ, Hancox JC.** Comparison of Na^+/Ca^{2+} exchanger current and of its response to isoproterenol between acutely isolated and short-term cultured adult ventricular myocytes. *Biochem Biophys Res Commun* 297: 302–308, 2002. doi:10.1016/S0006-291X(02)02200-3.
29. **Page E, Surdyk-Droske M.** Distribution, surface density, and membrane area of diadic junctional contacts between plasma membrane and terminal cisterns in mammalian ventricle. *Circ Res* 45: 260–267, 1979. doi:10.1161/01.RES.45.2.260.
30. **Pásek M, Brette F, Nelson A, Pearce C, Qaiser A, Christe G, Orchard CH.** Quantification of t-tubule area and protein distribution in rat cardiac ventricular myocytes. *Prog Biophys Mol Biol* 96: 244–257, 2008. doi:10.1016/j.pbiomolbio.2007.07.016.
31. **Pásek M, Simurda J, Orchard CH.** Effect of Ca^{2+} efflux pathway distribution and exogenous Ca^{2+} buffers on intracellular Ca^{2+} dynamics in the rat ventricular myocyte: a simulation study. *BioMed Res Int* 2014: 920208, 2014. doi:10.1155/2014/920208.
32. **Pott C, Yip M, Goldhaber JI, Philipson KD.** Regulation of cardiac L-type Ca^{2+} current in Na^+-Ca^{2+} exchanger knockout mice: functional coupling of the Ca^{2+} channel and the Na^+-Ca^{2+} exchanger. *Biophys J* 92: 1431–1437, 2007. doi:10.1529/biophysj.106.091538.
33. **Puglisi JL, Yuan W, Bassani JWM, Bers DM.** Ca^{2+} influx through Ca^{2+} channels in rabbit ventricular myocytes during action potential clamp: influence of temperature. *Circ Res* 85: e7–e16, 1999. doi:10.1161/01.RES.85.6.e7.
34. **Sako H, Sperelakis N, Yatani A.** Ca^{2+} entry through cardiac L-type Ca^{2+} channels modulates β-adrenergic stimulation in mouse ventricular myocytes. *Pflügers Arch* 435: 749–752, 1998. doi:10.1007/s004240050579.
35. **Scriven DRL, Moore EDW.** Ca^{2+} channel and Na^+/Ca^{2+} exchange localization in cardiac myocytes. *J Mol Cell Cardiol* 58: 22–31, 2013. doi:10.1016/j.yjmcc.2012.11.022.
36. **Sipido KR, Callewaert G, Carmeliet E.** Inhibition and rapid recovery of Ca^{2+} current during Ca^{2+} release from sarcoplasmic reticulum in guinea pig ventricular myocytes. *Circ Res* 76: 102–109, 1995. doi:10.1161/01.RES.76.1.102.

37. **Thomas MJ, Sjaastad I, Andersen K, Helm PJ, Wasserstrom JA, Sejersted OM, Ottersen OP.** Localization and function of the Na^+/Ca^{2+}-exchanger in normal and detubulated rat cardiomyocytes. *J Mol Cell Cardiol* 35: 1325–1337, 2003. doi:10.1016/j.yjmcc.2003.08.005.
38. **Trafford AW.** Location, location, location: new avenues to determine the function of the cardiac Na^+-Ca^{2+} exchanger? *J Mol Cell Cardiol* 35: 1321–1324, 2003. doi:10.1016/j.yjmcc.2003.09.005.
39. **Trafford AW, Díaz ME, Eisner DA.** Stimulation of Ca-induced Ca release only transiently increases the systolic Ca transient: measurements of Ca fluxes and sarcoplasmic reticulum Ca. *Cardiovasc Res* 37: 710–717, 1998. doi:10.1016/S0008-6363(97)00266-6.
40. **Trafford AW, Díaz ME, Negretti N, Eisner DA.** Enhanced Ca^{2+} current and decreased Ca^{2+} efflux restore sarcoplasmic reticulum Ca^{2+} content after depletion. *Circ Res* 81: 477–484, 1997. doi:10.1161/01.RES.81.4.477.
41. **Trafford AW, Díaz ME, O'Neill SC, Eisner DA.** Comparison of subsarcolemmal and bulk calcium concentration during spontaneous calcium release in rat ventricular myocytes. *J Physiol* 488: 577–586, 1995. doi:10.1113/jphysiol.1995.sp020991.
42. **Trafford AW, Díaz ME, Sibbring GC, Eisner DA.** Modulation of CICR has no maintained effect on systolic Ca^{2+}: simultaneous measurements of sarcoplasmic reticulum and sarcolemmal Ca^{2+} fluxes in rat ventricular myocytes. *J Physiol* 522: 259–270, 2000. doi:10.1111/j.1469-7793.2000.t01-2-00259.x.
43. **Walsh KB, Cheng Q.** Intracellular Ca^{2+} regulates responsiveness of cardiac L-type Ca^{2+} current to protein kinase A: role of calmodulin. *Am J Physiol Heart Circ Physiol* 286: H186–H194, 2003. doi:10.1152/ajpheart.00272.2003.
44. **Yang Z, Pascarel C, Steele DS, Komukai K, Brette F, Orchard CH.** Na^+-Ca^{2+} exchange activity is localized in the T-tubules of rat ventricular myocytes. *Circ Res* 91: 315–322, 2002. doi:10.1161/01.RES.0000030180.06028.23.